Applied Radiation and Isotopes 92 (2014) 91–95

Contents lists available at ScienceDirect

Applied Radiation and Isotopes

journal homepage: www.elsevier.com/locate/apradiso

# Photo-, cathodo- and thermoluminescent properties of dysprosium-doped $HfO_2$ films deposited by ultrasonic spray pyrolysis

R. Reynoso Manríquez [a], J.A.I. Díaz Góngora [a], J. Guzmán-Mendoza [a], T. Rivera Montalvo [a,*], J.C. Guzmán Olguín [a], P.V. Cerón Ramírez [a], M. García-Hipólito [b], C. Falcony [c]

[a] Centro de Investigación en Ciencia Aplicada y Tecnología Avanzada del Instituto Politécnico Nacional, Unidad Legaria, Calzada Legaria 694, Colonia Irrigación, C.P. 11500 México, D.F., Mexico
[b] Instituto de Investigaciones en Materiales, Universidad Nacional Autónoma de México, Circuito Exterior, Ciudad Universitaria, Coyoacán 04510, D.F., Mexico
[c] Centro de Investigación y de Estudios Avanzados del Instituto Politécnico Nacional, A.P. 14-740, México 07360, D.F., Mexico

## HIGHLIGHTS

- Luminescent properties of dysprosium doped hafnium oxide ($HfO_2$:$Dy^{3+}$) films were analyzed.
- $HfO_2$:$Dy^{3+}$ films were deposited by ultrasonic spray pyrolysis route.
- Emission spectra of $HfO_2$:$Dy^{3+}$ were analyzed by cathode and photoluminescence techniques.
- Luminescence mechanism in $HfO_2$:$Dy^{3+}$ was analyzed.
- Results of $HfO_2$:$Dy^{3+}$ suggest it as a good candidate as UVR dosimeter.

## ARTICLE INFO

*Article history:*
Received 12 March 2014
Received in revised form
20 May 2014
Accepted 5 June 2014
Available online 21 June 2014

*Keywords:*
Thermoluminescence
Luminescence
$HfO_2$:$Dy^{3+}$ films
Spray pyrolysis
UV radiation

## ABSTRACT

In this work, the photoluminescent (PL), cathodoluminescent (CL) and thermoluminescent (TL) properties of hafnium oxide films doped with trivalent dysprosium ions are reported. The films were deposited on glass substrates at temperatures ranging from 300 to 600 °C, using chlorides as precursor reagents. The surface morphology of films showed a veins shaped microstructure at low deposition temperatures, while at higher temperatures the formation of spherical particles was observed on the surface. X-ray diffraction showed the presence of $HfO_2$ monoclinic phase in the films deposited at temperatures greater than 400 °C. The PL and CL spectra of the doped films showed the highest emission band centered at 575 nm corresponding to the transitions $^4F_{9/2} \rightarrow {}^6H_{13/2}$, which is a characteristic transition of $Dy^{3+}$ ion. The greatest emission intensities were observed in samples doped with 1 atomic percent (at%) of $DyCl_3$ in the precursor solution. Regarding the TL behavior, the glow curve of $HfO_2$:$Dy^{+3}$ films exhibited spectrum with one broad band centered at about 150 °C. The highest intensity TL response was observed on the films deposited at 500 °C.



## 1. Introduction

The scientific investigation on luminescent materials has had a preponderant role along many years due to the great diversity of their possible technological applications (Lange et al., 2006; Khoshmann et al., 2008). The host matrix that contains the ions optically active in these luminescent materials can be constituted by metallic oxides, sulfides, selenides, etc. Among the metallic oxides, hafnium oxide ($HfO_2$) is a material with wide possibilities to be used as luminescent host matrix due to its physiochemical properties such as its high chemical stability, high melting temperature (2774 °C), high crystallographic density ($\approx 10\ g/cm^3$), energy band gap of 5.68 eV and a low phonon frequency. Also, experimental results show that the $HfO_2$ could be useful in UV radiation dosimetry applications (Balog and Schieber, 1977; Zhao and Vanderbilt; Chacón-Roa et al., 2008; García-Hipólito et al., 2004; Guzmán-Mendoza et al., 2010). Rare earths ions are considered as the most important luminescence activators for their narrow emission and absorption bands in the interval that goes

* Corresponding author.

http://dx.doi.org/10.1016/j.apradiso.2014.06.005
0969-8043/

from the UV–visible to the near infrared, due to type 4f→4f intraconfigurational transitions, which are weakly influenced by the crystalline field of the host. Many techniques are used to prepare hafnium oxide powders and films; these include atomic layer deposition, electron beam evaporation, ion-assisted electron beam deposition, chemical vapor deposition and the sol–gel method (Ho et al., 2003; Chow et al., 1993; Al-Kuhaili et al., 2004; Lehan et al., 1991; Gilo and Croitoru., 1999; Baumeister and Arnon, 1977; LeLuyer et al., 2008), etc. However, the ultrasonic spray pyrolysis technique has proved to be an efficient and low cost technique to synthesize films of metallic oxides. Due to their relative simplicity and the possibility of being scalable at industrial level, this process has been used for obtaining films and powders for optical, semiconductor, and magnetic applications (Kang and Lenahanm, 2003; Villanueva-Ibañez et al., 2003). In this work, we use the ultrasonic spray pyrolysis process to deposit undoped $HfO_2$ films and optically activate it with $Dy^{3+}$ ions ($HfO_2$:$Dy^{3+}$). To our best knowledge, the PL, CT and TL properties of $Dy^{3+}$ doped hafnium oxide films, deposited by the ultrasonic spray pyrolysis process, had not been systematically studied.

## 2. Experimental

The undoped $HfO_2$ and Dy doped $HfO_2$ films ($HfO_2$:$Dy^{3+}$) were deposited by the ultrasonic spray pyrolysis technique on Corning 7059 glass slides substrates. The starting reagents were $HfCl_2O{\bullet}8H_2O$ (98%) and $DyCl_3{\bullet}XH_2O$ (99%) (Alfa-Aesar) dissolved in deionized water at a molar concentration of 0.05 M. Substrate temperatures ($T_s$) during deposition were in the range from 300 °C to 600 °C with steps of 100 °C. The carrier gas flow (filtered air) was 10 l/min. The $DyCl_3{\bullet}XH_2O$ concentration in the spraying solution was in the range from 0 to 20 at% in relation to the hafnium content. The deposition time was adjusted to 10 min, in order to obtain similar thickness of all samples. This thickness was approximately $10 \pm 0.03$ μm as measured by a Sloan Dektak IIA profilometer. Structural properties of the films were determined by means of the X-ray diffraction technique (XRD) using a Siemens model D-500 diffractometer, with a $Cu_{K\alpha}$ radiation ($\lambda = 1.5406$ Å). The surface morphology was analyzed with a Cambridge-Leica model Stereo-Scan 440, scanning electron microscope (SEM) and the chemical elements inside the films were measured by energy dispersive spectroscopy (EDS) with an Oxford Si–Li X-ray detector model Pentafet, coupled to the above microscope. The PL properties were measured with a spectrofluorimeter Fluoro Max®-P, using a Xenon (Xe) lamp as an excitation source. CL measurements were performed in a stainless steel vacuum chamber with a cold cathode electron gun (Luminoscope, model ELM-2 MCA, RELION Co.). The samples were placed inside the vacuum chamber which was evacuated to 10 mTorr. The emitted light from the sample was coupled into an optical fiber bundle which was lead to the previously mentioned spectrophotometer. Previous to the determination of TL characteristics, the films were subjected to thermal annealing treatment at 300 °C during 10 min in order to erase any remaining information. After this process, the samples were irradiated individually with UV radiation at different wavelengths (200–400 nm) using a Xe lamp coupled to a monochromator Newport Oriel Apex model 70510 model 74125. TL glow curves of $HfO_2$:$Dy^{+3}$ were recorded using a Harshaw TLD reader (Model 3500). The TL signal was integrated from 50 °C to 400 °C using a heating rate of 10 °C $s^{-1}$. All TL measurements were obtained in a nitrogen atmosphere in order to reduce the thermal noise resulting from the heating planchet of the TL reader.

## 3. Results and discussion

The surfaces morphology of $HfO_2$ films is presented in Fig. 1. The film deposited at 300 °C (Fig. 1a) has a porous surface with a veins shaped microstructure having a uniform distribution of material deposited on the whole substrate. These physical characteristics of the films deposited at low temperatures can be attributed to the spray impinges on the hot substrate in liquid form; in this case, the thermal energy is not enough to process the material completely and to form closed and compact surfaces. The surface of the films deposited at higher temperatures appears more compact, with less porosity and with the formation of some spherical structures on the surface (Fig. 1b). This microstructure is probably the result of a greater superficial kinetic energy of precursor species due to the increment in substrate temperature. In all films deposited at temperatures below 500 °C rough but continuous films with good adherence to the substrate are observed. Fig. 1c shows the surface of the film deposited at 600 °C. This micrograph shows a surface constituted by a great quantity of clusters formed by particles of spherical shape; some regions where the film loses continuity can be observed. Fig. 1d shows the SEM micrograph with a cross section view of the sample deposited at 600 °C a nodular growth of the films with a thickness of approximately 10 μm and with a microstructure constituting of hollow spherical particles with diameters of approximately 2 μm can be observed.

The SEM micrographs show that all films, independent of their substrate temperature, have morphologies with a great superficial area, which is advantageous for some applications. The relative atomic percentages of oxygen, hafnium, dysprosium, and chlorine inside the films, as a function of deposition temperature and the doping concentration, were obtained by EDS. The samples deposited at 600 °C show a ratio of oxygen/hafnium close to 2, which is the theoretical value for a stoichiometric relation of the hafnium oxide. The samples deposited at 300 °C showed significant amount of chlorine (~20.0 at%); however, this concentration diminishes notably as the deposition temperature increases up to 600 °C, reaching a minimum value of 4 at%. This behavior can be explained if we consider that when the substrate temperature increases it promotes a greater dissociation and evaporation of species related with the precursor elements; probably here it promotes the formation of more quantity of gaseous HCl, which prevents the incorporation of the chlorine inside the films. On the other hand, as the substrate temperature increases, the films obtain a better crystalline structure which could prevent the incorporation of the chemical species related to chlorine. The XRD measurements corresponding to $HfO_2$ films deposited at substrate temperatures lower than 400 °C showed the absence of diffraction peaks, indicating that at these substrate temperatures the deposited material has a non-crystalline phase. On the other hand, XRD spectra corresponding to films deposited at greater substrate temperature than 500 °C showed defined peaks, indicating that films acquired a crystalline structure. The decrease in the width of the peaks, as temperature increases, indicates an increment in the crystal sizes of the films. The diffractogram of film deposited at 600 °C with Miller indexes of corresponding planes is shown in Fig. 2. This peak appropriately corresponds to hafnium oxide monoclinic phase (PCPDFWIN card file number 340104).

The crystallites size, in the film deposited at 600 °C, was estimated by means of Scherrer's equation, considering the most intense peak is located at 28.43°, corresponding to the plane (−111). The obtained size of crystallites was 15 nm. In the PL characterization of the $HfO_2$:$Dy^{3+}$ films, the emission and excitation spectra as a function of the substrate temperature and doping concentration were obtained. The inset in Fig. 3 shows the excitation spectrum of the film deposited at 600 °C with $Dy^{3+}$

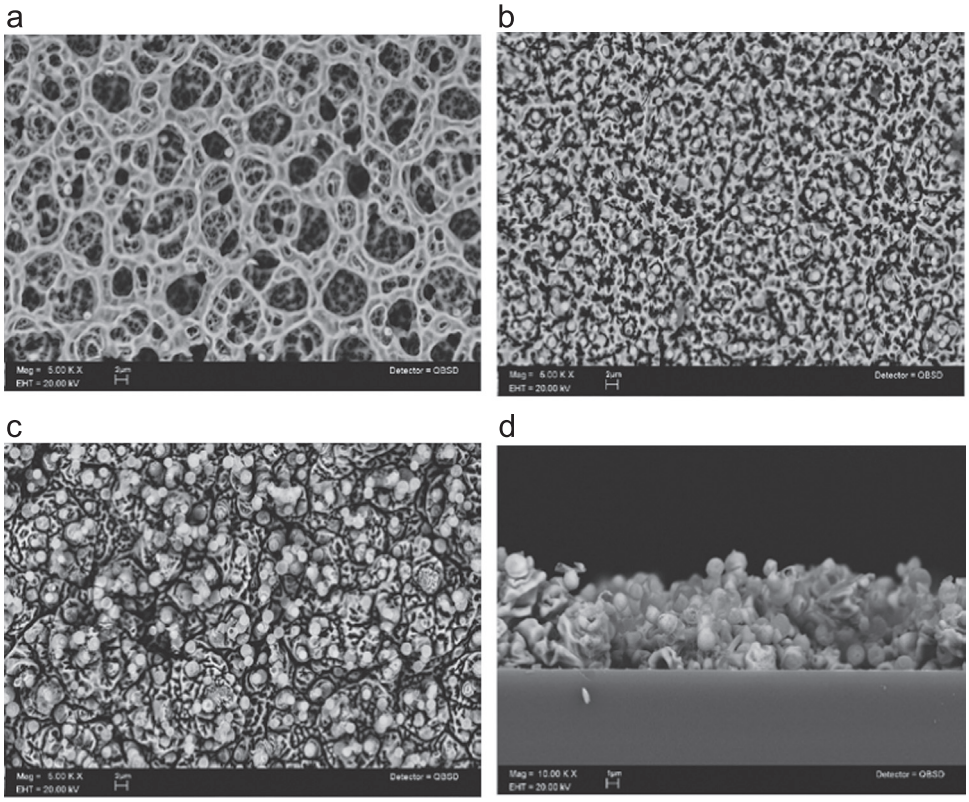


**Fig. 1.** Microstructure of the undoped $HfO_2$ films deposited at 300 °C (a), 400 °C (b), 600 °C (c) and cross section view of the film deposited at 600 °C (d).

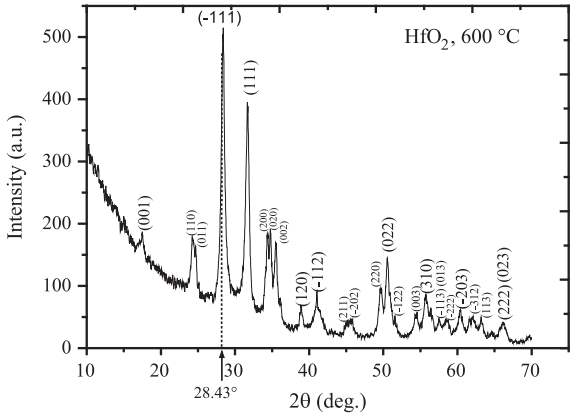


**Fig. 2.** XRD pattern with Miller index of the undoped $HfO_2$ film deposited at 600 °C.

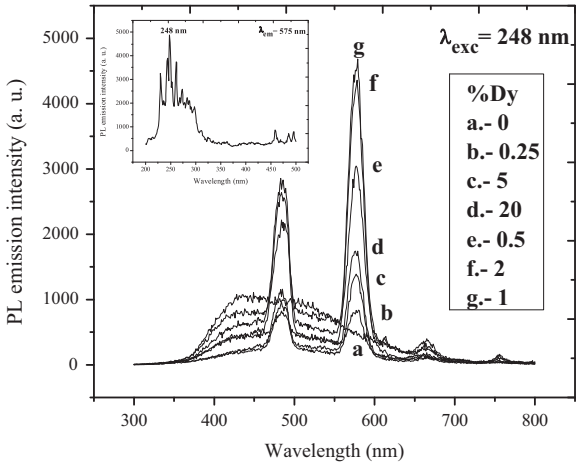


**Fig. 3.** PL emission spectra of $HfO_2$:Dy films deposited at 600 °C as a function of the doping concentration. The excitation wavelength was 248 nm. The inset corresponds to the PL excitation spectrum for a $HfO_2$:Dy (1 at%) film, deposited at 600 °C. The excitation spectra were recorded with $\lambda_{emi}$=575 nm.

(1 at%). The emission wavelength ($\lambda_{em}$) was fixed at 575 nm, which corresponds to the band with maximum intensity in the $Dy^{3+}$ emission spectrum. This spectrum shows two groups of bands; one of them shows some peaks between 230 nm and 300 nm. The other group shows bands between 450 nm and 500 nm. The peaks observed below 300 nm are usually related to 4f–5d transitions or Dy–O charge transfer bands and above 300 nm are related to 4f–4f transitions. The most intense peak in this spectrum corresponds to 248 nm, which was selected as an excitation wavelength to obtain the PL emission spectra.

The PL emission spectra for $HfO_2$:$Dy^{3+}$ films deposited at 600 °C, with different activator concentrations, are shown in Fig. 3. In this spectrum, it is possible to observe four bands centered at 480, 575, 658 and 747 nm, which correspond to the electronic transitions $^4F_{9/2}\rightarrow{}^6H_{15/2}$, $^4F_{9/2}\rightarrow{}^6H_{13/2}$, $^4F_{9/2}\rightarrow{}^6H_{11/2}$ and $^4F_{9/2}\rightarrow{}^6H_{9/2}$, respectively, characteristic of $Dy^{3+}$ ion (Chase et al., 1969). It can be observed that PL emission intensity increases until it reaches a maximum of 1 a/o for $Dy^{3+}$ ions in the precursor solution. After this value, a decrease of PL emission intensity is shown due to the excess of activators; this effect is known as the concentration quenching. In the literature, Dexter and Schulman have suggested that, at high impurities concentration, the excitation energy can migrate from one luminescent center to another and eventually reach a sink, from which nonradiative processes can dissipate this excitation energy. This concentration quenching will not appear at low concentrations because the average distance between activators is so large that the migration of excitation energy is prevented and the sink is not reached (Dexter and Schulman, 1954). Fig. 4 shows PL emission spectra for $HfO_2$:$Dy^{3+}$

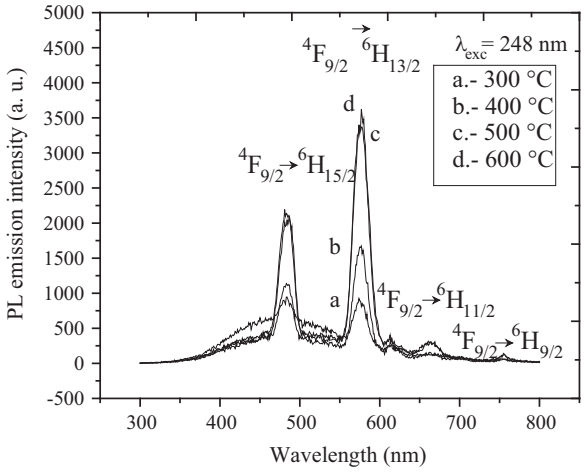


**Fig. 4.** PL emission spectra of $HfO_2$:Dy (1 at%) films at different substrate temperatures. In this case, the wavelength of excitation was 248 nm.

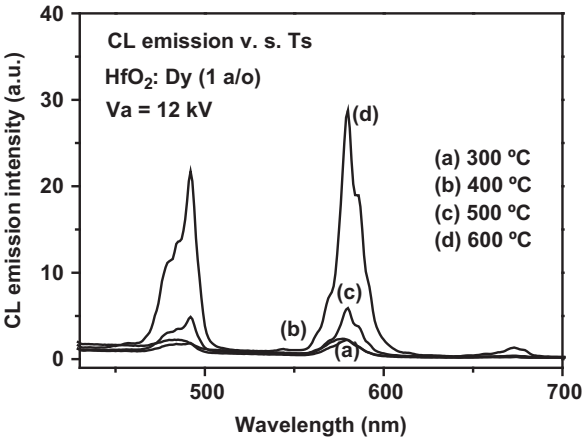


**Fig. 5.** CL emission spectra of $HfO_2$:Dy (1 at%) films with variations of the substrate temperature. The electron accelerating voltage was 12 kV.

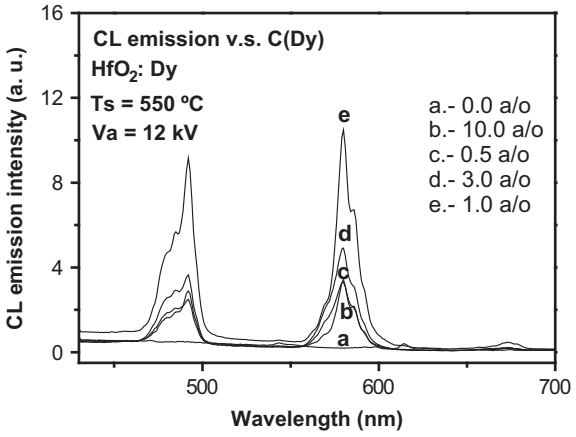


**Fig. 6.** CL emission spectra of $HfO_2$:Dy films deposited at 600 °C, as a function of doping concentration. In this case, the electron accelerating voltage was 12 kV.

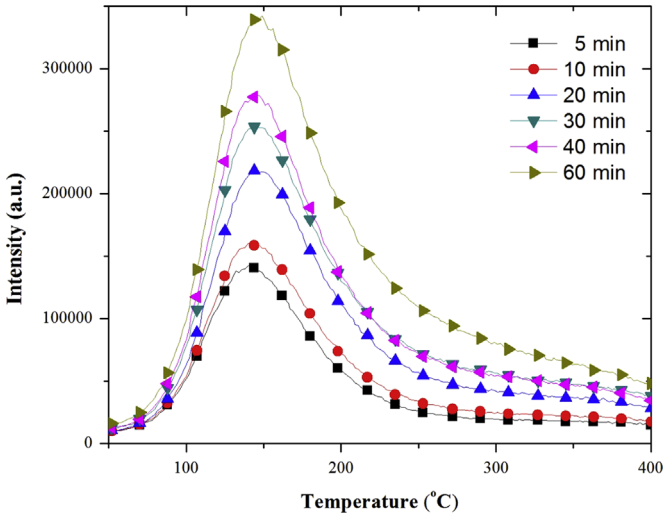


**Fig. 7.** TL response of $HfO_2$:Dy (1 at%) films, deposited at 500 °C.

(1 at%) films as a function of substrate temperature. The spectra show the effect of the deposition temperature on the PL emission intensity. It is possible to observe that the PL emission intensity is favored with the rise in substrate temperature.

The higher PL emission intensity corresponds to films deposited at 600 °C. According to the XRD measurements the films deposited at high substrate temperatures show structures with a better crystallinity; as a consequence, the $DY^{3+}$ ions are optimally distributed and incorporated in the host lattice, since the distance between them is sufficiently large enough to avoid transfer of the energy among them. A strong yellowish-white PL emission is observed by the naked eye in normal room light when the films are excited with a 4 W UV–mercury lamp (254 nm). Fig. 5 shows the CL emission spectra of $HfO_2$:$Dy^{3+}$ films, at different substrate temperatures. The electron accelerating voltage (Va) was 12 kV and the doping concentration in the spraying solution was fixed at 1 at% of $DyCl_3$. These spectra show dominant bands centered at 490 nm, 580 nm and a small peak localized at 673 nm, which correspond, as in the case of PL measurements, to the electronic transitions $^4F_{9/2} \rightarrow {}^6H_{15/2}$, $^4F_{9/2} \rightarrow {}^6H_{13/2}$, and $^4F_{9/2} \rightarrow {}^6H_{11/2}$ of the $Dy^{+3}$ ions, respectively. Once again (as in PL measurements) the strongest emission corresponds to yellow $^4F_{9/2} \rightarrow {}^6H_{13/2}$ electronic transition. It is clear that the CL emission intensities rise with increasing substrate temperature, suggesting that a reduction of structural defects and the crystallite growth in the films favors the radiative recombination mechanisms. Probably the reduction of residual impurities (as chlorine) incorporated into the crystallized samples produces a better incorporation and distribution of $Dy^{3+}$ ions into the host lattice, which would result in an increase of the CL intensity as the deposition temperature is increased.

The CL emission spectra for $HfO_2$:$Dy^{3+}$ film, as a function of the doping concentration for the films deposited at 600 °C with an applied electron accelerating potential of 12 kV, are shown in Fig. 6. It is possible to observe the same behavior as in the PL spectrum, as the $DyCl_3$ concentration is increased, because a quenching effect of the overall CL emission is observed; the maximum emission intensity was obtained for 1 a/o of $DyCl_3$ in the precursor solution. When using rare-earth as activators, the migration of the energy of excitation by resonant energy transfer between the rare-earth activators can be so efficient in that it may carry the excitation energy to a sink; thus the aggregation of activator ions at high concentration may change some activators to quenchers and induce the concentration quenching effect (Hase et al., 1990). The CL spectra with different accelerating voltages in the range from 3 to 12 kV were also acquired for these films. It was possible to observe that the overall emission intensity is larger for higher electron accelerating voltage showing no saturation effect in the voltage range studied. In principle, the incident electron beam reaches and penetrates the luminescent films to generate

secondary electrons and electron–hole pairs which excite the activator ions in the host lattice and generate CL emissions. As the electron accelerating voltage increases, the penetrating electrons produce more electron–hole pairs due to the interaction with a larger volume, resulting in much more intense activator luminescence due to the recombination of the electron–hole pairs.

Fig. 7 shows the TL glow curves of the $HfO_2$:$Dy^{3+}$ films exposed to UV radiation at different spectral irradiance (irradiation times). The TL response was evaluated from the total area under the glow curve, after background subtraction, where the highest TL response was obtained in the film deposited at 500 °C. All TL glow curves exhibited in Fig. 7 are results of UVR interaction on the samples. As it can be seen that the curves have a broad peak centered at around 150 °C; the width of the peaks suggests a continuous distribution of the tramps. This glow curve is the final result after subtraction from natural radiation contribution and the substrate contribution (substrate contribution was very lower in all experiments). The increase in the intensities of the glow peaks with increase of dose can be understood by the fact that more and more active centers were activated. The TL response of $HfO_2$:$Dy^{3+}$ as a function of the exposition time with a wavelength of UV radiation of 240 nm was analyzed in a wide range and showed an almost linear response from 24 to 288 mJ/cm$^2$. This linearity suggests the possible use of $HfO_2$:$Dy^{3+}$ as a dosimeter in the environmental UV radiation monitoring.

## 4. Conclusions

By means of the ultrasonic spray pyrolysis process it was possible to synthesize $HfO_2$ films doped with $Dy^{3+}$ ions. The surface morphology of the films was dependent on the substrate temperature; SEM images showed that these films are rough but continuous and denser as the deposition temperature is increased. The obtained films show a uniform growth of material in the whole area of the substrate. The films showed high superficial area and high roughness (2–3 μm), with an average thickness of 10 μm. The crystalline structure of the analyzed films depended on the substrate temperature; at low temperatures they are in an amorphous state and when the deposition temperature is increased they are transformed, mainly to a polycrystalline monoclinic phase of the $HfO_2$, with an estimated crystal size of 15 nm. From the excitation spectrum it was determined that optimum wavelength to excite the luminescent films was 248 nm. In addition, a concentration quenching was observed and the optimum $DyCl_3$ concentration was 1 a/o in the deposition solution. It was also determined that substrate temperature for the sample with maximum PL emission intensity was 600 °C. The PL (yellowish-white emission) is intense since it can be observed by the naked eyes with normal ambient illumination when excited with a portable mercury lamp with a wavelength of 254 nm. This gives an idea, if not quantitatively at least qualitatively, of the strength of the PL emission. Similar results to those of PL were obtained in the case of CL. Concerning the TL response of samples under UVR radiation a good TL response was exhibited. Fig. 7 shows a broad glow curve for the sample exposed by UVR which is the overlapping of two peaks if a deconvolution process is applied. Then, these three experimental characterization techniques show two maximum emission centers for $HfO_2$:$Dy^{3+}$. Finally, once again, it was confirmed that hafnium oxide is an adequate host matrix for rare earth ions (in this case $Dy^{3+}$) and as active centers to generate strong yellowish-white PL, CL and TL emissions.

## Acknowledgments

The authors wish to thank the SIP-IPN for the financial support through the Project 20140503 and Grand CONACYT Project 223069. Also, we would like to thank Adriana Tejeda, Omar Novelo, Zacarías Rivera and Marcela Guerrero for technical support.

## References

Al-Kuhaili, M.F., Durrani, S.M.A., Khawaja, E.E., 2004. J. Phys. D: Appl. Phys. 37, 1254–1261.
Balog, M., Schieber, M., 1977. Thin Solid Films 41, 247–259.
Baumeister, P., Arnon, O., 1977. Appl. Opt. 16 (2), 439–444.
Chacón-Roa, C., Guzmán-Mendoza, J., Aguilar-Frutis, M., García-Hipólito, M., Alvarez-Fragoso, O., Falcony, C., 2008. J. Phys. D: Appl. Phys. 41 (015104) (7pp).
Chase, E.W., Hepplewhite, R.T., Kruoka, D.C., Kahng, D., 1969. J. Appl. Phys. 40 (6), 2512–2519.
Chow, R., Falabella, S., Loomis, G.E., Rainer, F., Stolz, C.h.J., Kozlowski, M.R., 1993. Appl. Opt. 32 (28), 5567–5574.
Dexter, D.L., Schulman, J.H., 1954. J. Chem. Phys. 22, 1063.
García-Hipólito, M., Alvarez-Fregoso, O., Guzmán, J., Martínez, E., Falcony, C., 2004. Phys. Stat. Sol. A 201 (15), R127–R130, http://dx.doi.org/10.1002/pssa.200409076.
Gilo, M., Croitoru, N., 1999. Thin Solid Films 350, 203–208.
Guzmán-Mendoza, J., Aguilar-Frutis, M., Alarcón Flores, G., García-Hipólito, M., Maciel Cerda, A., Azorín Nieto, J., Rivera Montalvo, T., Falcony, C., 2010. Appl. Radiat. Isot. 68, 696–699.
Hase, T., Kano, T., Nakasawa, E., Yamamoto, H., 1990. Phosphors materials for cathode-ray tubes. Advances in Electronics and Electron Physics, vol. 79. Academic Press, Elsevier Inc. p. 271.
Ho, M.Y., Gong, H., Wilk, G.D., Busch, B.W., Green, M.L., Voyles, P.M., Muller, D.A., Bude, M., Lin, W.H., See, A., Loomans, M.E., Lahiri, S.K., Räisänen, Petri I., 2003. J. Appl. Phys. 93 (3), 1477–1481.
Kang, A.Y., Lenahanm, P.M., 2003. Appl. Phys. Lett. 83 (16).
Khoshmann, J.M., Khan, A., Kordesch, M.E., 2008. Surf. Coat. Technol. 202, 2500–2502.
Lange, S., Kiisk, V., Reedo, V., Kirm, M., Aarik, J., Sildos, I., 2006. Opt. Mater. 28, 1238.
LeLuyer, C., Villanueva-Ibañez, M., Pillonnet, A., Dujardin, C., 2008. J. Phys. Chem. A 112, 10152–10155.
Lehan, J.P., Mao, Y., Bovard, B.G., Macleod, H.A., 1991. Thin Solid Films 203, 227–250.
Villanueva-Ibañez, M., Dujardin, C., Mugnier, J., 2003. Mater. Sci. Eng. B 105, 12–15.
Zhao, X., Vanderbilt, D., 2002. Phys. Rev. B 65, 2331056.